Fragmentation of kimberlite: insights into eruption style and energy from Diavik, NWT

S. Moss (1,2), J.K. Russell (1,2), R. Brett (1), G.D.M. Andrews (1,2)

(1) Volcanology and Petrology Lab, University of British Columbia, British Columbia, Canada, (2) Mineral Deposit Research Unit, University of British Columbia, British Columbia, Canada

1. Introduction

One metric of the intensity of a volcanic eruption is the extent of magma fragmentation as recorded by pyroclasts. Relative comparisons of volcanic energy are made for historical eruptions by using the combination of grain size distributions and areal extent of pyroclastic deposits. For example, 'F' values which represent the % of fragments < 1 mm at isopach contour of 0.10 $Thickness_{max}$ are used for comparative purposes and to deduce volcanic style and energy from grain-size properties of pyroclastic deposits (Walker, 1973; Cas and Wright, 1987). Kimberlite volcanoes rarely preserve extra-crater deposits that would support this type of analysis. Furthermore, many volcaniclastic deposits of kimberlite are enriched (> 50%) in crystals (e.g., olivine) and, thus, the energetics behind fragmentation of crystal-rich kimberlite magmas may be considerably different from other magmas.

Melt-free olivine crystals and juvenile pyroclasts of crystallized kimberlite magma +/- olivine crystals are the dominant pyroclast types in kimberlite. Any estimation of kimberlite eruption intensity from deposits must also consider the properties of these components. Here we present data collected from coherent and pyroclastic kimberlite within a kimberlite pipe at Diavik, NWT. We use these data to test the following hypotheses: (a) olivine crystals fragment during explosive eruption of kimberlite; (b) explosive eruption of kimberlite commonly separates kimberlite melt from olivine crystals. Our analysis also suggests that size distribution of olivine crystals and the nature of juvenile pyroclasts are indicative of the relative intensity of kimberlite eruptions. On that basis, we present a new fragmentation index for kimberlite eruption using a.) crystal sizes in olivine populations and b.) ratios of 'free' olivines to juvenile olivine-phyric pyroclasts.

2. Diavik context

The focus of this study is the A154N kimberlite pipe at Diavik, NWT (Figure 1). The A154N pipe contains $6.2x10^6 m^3$ of kimberlite comprising multiple volcanic facies: pyroclastic kimberlite (PK1,PK2), resedimented volcaniclastic kimberlite (RVK), and coherent kimberlite (CK) as dykes intruding fragmental pyroclastic kimberlite in the pipe interior (Moss et al., 2008). To test the hypotheses stated above, we have collected and analyzed modal abundances and crystal size distributions of olivine in pyroclastic kimberlite (PK2) and coherent kimberlite (CK) from A154N. The PK2 deposit fills the uppermost 50m of the A154N pipe, and is interpreted as a pyroclastic density current of kimberlite sourced from outside A154N which was deposited into a deep crater lake (Moss et al., 2008).

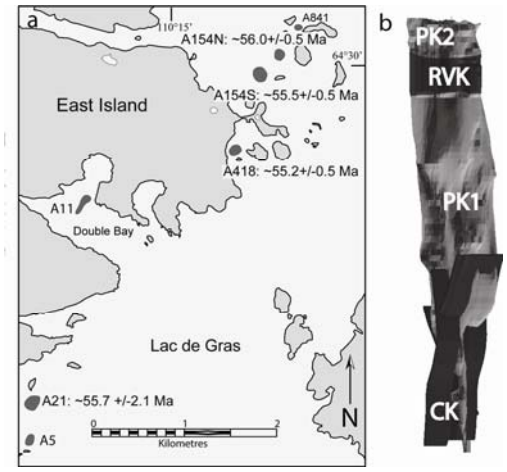

Figure 1: Diavik, NWT. (a) East Island on Lac de Gras, NWT, showing locations and ages of kimberlite pipes. (b) 3-D model of A154N showing locations of pyroclastic kimberlite (PK1,PK2), resedimented volcaniclastic kimberlite (RVK), and coherent kimberlite (CK).

3. Hypothesis 1: Olivines break during eruption

Crystal size distributions (CSDs) are collected by image analysis of olivine particles in 2-D sections of polished slabs and thin sections using techniques outlined in Moss et al. (2008). CSD's of olivine crystals in coherent kimberlite (CK) from multiple dykes intruding into the base of the A154N kimberlite pipe are compared with CSDs of olivine crystals from pyroclastic rocks (PK) in A154N in Figure 2a,b. For both CK olivines and PK olivines, sizes (as cut section area) consistently range from 0.001 to ~100mm^2. However, the relative proportions of size ranges of most olivine (0.01-10mm^2) between CK and PK show significant variation. For example, 50% of CK olivines comprise crystals > 2mm^2, while 50% of PK olivines are > 0.5mm^2 (Figure 2a). Thus, our data show an

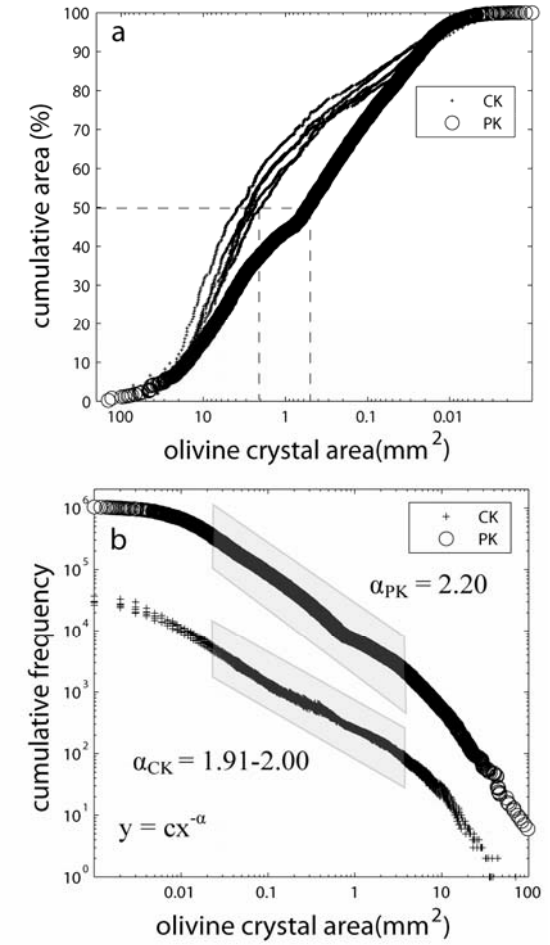

Figure 2: Olivine crystal size distribution data from CK and PK of A154N. (a) Cumulative area (as %) vs. olivine crystal area (mm^2) for 5 samples of CK and from 1 PK deposit. PK olivine data represents amalgamation of olivine crystal sizes from 20 samples within the PK. Data from two scales of observation is normalized to the largest scale, and linearly combined due to the systematic vertical grading of the deposit (Moss et al., 2008). (b) Cumulative frequency vs. olivine crystal area (mm^2) for samples from (a).

overall disparity in crystal sizes between the two facies (Figure 2a,b). Characterizing crystal and clast populations using model distributions can be helpful in deducing eruption process (e.g. Kaminski and Jaupart, 1998). Recent investigations, however, show that many distributions reported to obey power-laws can be explained by other models (Clauset et al., 2007). Here we apply distribution-fitting tests (after Clauset et al., 2007) on crystal sizes within 2σ of mean sizes in CK and PK (shaded regions; Figure 2b). Analysis of olivine data from CK and PK indicate a power-law distribution ($y = cx^{-\alpha}$) is a plausible fit to the data (goodness of fit $d_{CK} = 0.04$, $d_{PK} = 0.21$, where 0 means the model is a perfect fit). Power-law exponents of olivines reveal a shift from coherent facies (α_{CK} = 1.91-2.00) to pyroclastic facies (α_{PK} = 2.20).

Table 1: Representative olivine content* in coherent kimberlite (CK), pyroclastic kimberlite (PK) and juvenile pyroclasts (JP) of crystallized kimberlite

sample	% ol	% gm	A_{OL} : A_{GM}	% 'free' ol	% jp	A_{OL} : A_{JP}
CK 01†	40.5	52.1	0.8			
CK 02b†	46.0	45.6	1.0			
CK 03†	47.4	45.2	1.0			
CK_06	53.5	42.6	1.3			
CK_08	62.1	30.1	2.1			
CK_TOT	49.9	43.1	1.2			
PK 330‡				26.9	3.9	6.9
PK 340‡				53.2	2.3	22.9
PK 350‡				56.9	1.3	43.8
PK 360‡				26.1	5.1	5.1
PK 37‡				32.9	5.2	6.3
PK 380‡				35.2	18.2	1.9
PK_TOT§				35.8	5.4	**6.7**
JP_TOT‖	66.3	33.7				2.0
PKJP_TOT¥	39.4	1.8	22.4			

* olivine content measured as area % from slab and t.s.
† Replicate samples from a single dyke; melt = groundmass
‡ Representative sample horizons within 50m-thick PK
§ Linear combination of 10 samples at 5m intervals in PK
‖ Linear combination of olivine in juvenile pyroclasts (jp) from PK
¥ Combined modal % of olivine in PK and resident jp in PK

4. Hypothesis 2: Kimberlite melt can efficiently separate from olivine crystals during eruption

To test this hypothesis, we again use image analysis to obtain relative modal proportions of olivine:melt in the CK, PK, and juvenile pyroclasts from the PK. Results are summarized in Table 1. Olivine crystal to groundmass ratios are ~1:1 in CK; 'free' crystals to olivine-phyric juvenile pyroclasts ~6.5:1 in PK. Combining the proportions of liberated olivine grains with those enclosed in juvenile pyroclasts yields a total olivine crystals : melt ratio of >20. If PK is the result of disruption of CK, there are two implications. First, the high proportion of free olivine grains indicates that explosive eruption of kimberlite is an efficient vehicle for separating crystals from melt. Second, the very high crystal:melt ratios (i.e., > 20) require substantial loss of the melt fraction during transport, eruption, and deposition; the solid content nearly doubles in pyroclastic deposits relative to coherent kimberlite.

5. Controls on olivine-breaking during eruption

The capacity of olivine crystals to resist fragmentation during eruption is a function of the intrinsic properties of olivine, the properties of the melt phase, and the original crystal size. Intrinsic properties of olivine crystals affecting breakage include stored strain in crystals, tensile strength (τ_{ol}) and the presence of fluid inclusions. Melt properties which affect how crystals break include the surrounding overpressures in the gas/melt/fluid mixture, the amount of melt surrounding or adhering to a crystal during eruption,

and the flow regime of the erupting magma (laminar vs. turbulent). Differences in CSD curves for CK and PK suggest size fractions most susceptible to grain size reduction are 0.03-10mm^2; coarse sizes (>10mm^2) and the smallest size fraction (<0.03mm^2) may be preserved during fragmentation processes (Figure 2a). Assuming the CK has the same olivine content as the parental magma responsible for the PK, we interpret the grain size disparity apparent in Figure 2 to be a direct result of eruption processes, and therefore a process-driven *reduction* in measured crystal sizes. Furthermore, olivines CSDs in coherent kimberlite possess characteristic slopes, (e.g. α_{CK} vs. α_{PK}, Figure 2b) and could be compared with those observed for olivines in pyroclastic rocks to index relative changes in populations due to eruption and/or secondary transport processes.

6.0 Controls on melt disruption

Kimberlite is presumed to be a low-viscosity, volatile-rich melt (Sparks et al., 2006). Its high volatile content could lead to very high exit velocities for the gas phase. The high density of the pyroclasts involved in a kimberlite eruption (e.g. Sparks et al., 2006; Moss et al., 2008,) would severely limit the exit velocity of solid particulate matter being ejected from a vent. The collective behaviors of gas and solid particles in a vent undergoing a flux of melt+solids+gas would yield a substantial but highly variable velocity contrast between phases. This Δv, coupled with the low viscosity and potential shear-thinning behavior of kimberlite melt could create instabilities on the gas:liquid interface (e.g. Reinhold-Helmholz, Rayleigh-Taylor), leading to substantial disruption (i.e. spray or jet) of the melt phase of kimberlite (i.e. We$_c$[1] >> 1), efficient separation of melt from crystals, and elutriation of the fine fraction of erupted products (ash). Thus, velocity contrasts (Δv) between gas and solid particles in the erupting magma may be manifested in the relative ratios of juvenile pyroclasts of crystallized melt (+/- enclosed olivine crystals) to 'liberated' or cognate olivine crystals observed in a deposit. We suggest that gas:liquid:solid ratios determine how readily melt can separate from crystals. For example, high gas : (liquid + solids) would readily separate melt from crystals. Conversely, high crystal : melt ratios (i.e., high modal % olivine) likely hinder efficient separation, and separation may be affected by the size distribution of crystals enclosed in the melt.

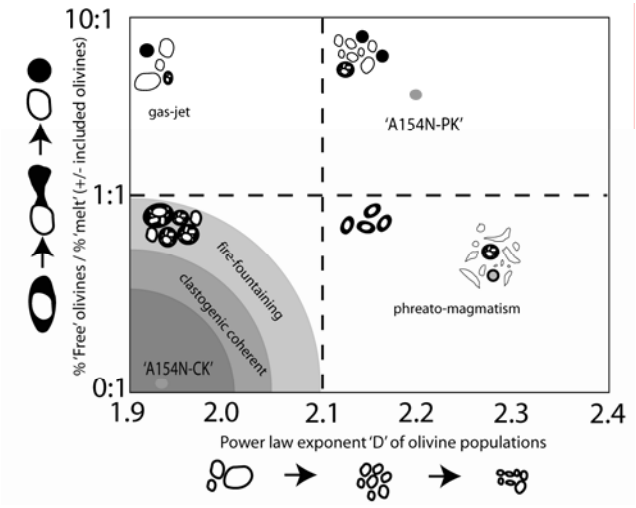

Figure 3: Proposed relative index of fragmentation for kimberlite eruptions. Modal abundance and CSD data for olivine crystals from deposits at A154N at Diavik (PK2,CK) are used to establish limits for melt separation (% free olivines : % melt) and crystal breaking (power law exponents) parameters.

7.0 Index of Fragmentation in kimberlite eruptions

These observations and data are used to propose a relative index of fragmentation intensity for kimberlite eruptions (Figure 3). Dimensionless ratios of melt separation (% 'free' olivines **:** % juvenile pyroclasts +/- enclosed olivine crystals) are plotted against power-law exponents of olivines crystal size distributions using data from known and hypothetical deposits of pyroclastic kimberlite. The resulting plot allows for (a) characterization of eruption intensity observed among the variety of intra- and extra-crater pyroclastic deposits of kimberlite worldwide, and (b) for the identification of unique explosive/fragmentation events or units within a pipe.

Cas, R.A.F. and Wright, J.V., 1987. Volcanic successions, modern and ancient. Chapman & Hall, London, 528 pp.

Clauset, A., Shalizi, C.R. and Newman, M.E.J., 2007. Power-law distributions in empirical data. arXiv 0706_1062v1, 1-26.

Kaminski, E. and Jaupart, C., 1998. The size distribution of pyroclasts and the fragmentation sequence in explosive volcanic eruptions. Journal of Geophysical Research 103((B12)), 29759–29779.

Moss, S., Russell, J.K. and Andrews, G.D.M., 2008. Progressive infilling of a kimberlite pipe at Diavik, Northwest Territories, Canada: Insights from volcanic facies architecture, textures, and granulometry. Journal of Volcanology and Geothermal Research 174.

Sparks, R.S.J., Baker, L., Brown, R.J., Field, M., Schumacher, J., Stripp, G. and Walters, A., 2006. Dynamical constraints on kimberlite volcanism. Journal of Volcanology and Geothermal Research 155(1-2), 18-48.

Walker, G.P.L., 1973. Explosive volcanic eruptions--A new classification scheme. Geol Rudsch 62, 431-446.

[1] Critical Weber numbers (We$_c$) mark the onset of 'bag' breakup in liquids (atomization), and have been shown to vary with viscosity. $We = p_g(\Delta v)^2(d_0/\sigma)$, where p_g is gas density, Δv is relative velocity between liquid and gas, d_0 is liquid droplet diameter, and σ is surface tension.